

Appendix

Bacterial FtsZ protein forms phase-separated condensates with its nucleoid-associated inhibitor SlmA

Begoña Monterroso^{1,4*}, Silvia Zorrilla^{1,4*}, Marta Sobrinos-Sanguino¹, Miguel A. Robles-Ramos¹, Marina López-Álvarez¹, William Margolin², Christine D. Keating³, Germán Rivas^{1*}

¹Centro de Investigaciones Biológicas, Consejo Superior de Investigaciones Científicas (CSIC) 28040, Madrid, Spain; ²Department of Microbiology and Molecular Genetics, McGovern Medical School, University of Texas, Houston TX, 77030, USA; ³Department of Chemistry, Pennsylvania State University, University Park, Pennsylvania 16802, USA.

⁴These authors contributed equally to this work.

*For correspondence: monterroso@cib.csic.es (BM), silvia@cib.csic.es (SZ), grivas@cib.csic.es (GR).

Table of contents	Page
Figure S1	A2
Figure S2	A2
Figure S3	A2
Figure S4	A3
Figure S5	A4
Figure S6	A4
Figure S7	A4
Figure S8	A5
Figure S9	A5
Figure S10	A5
Figure S11	A6
Figure S12	A6
Figure S13	A7
Figure S14	A7
Figure S15	A8
Figure S16	A8

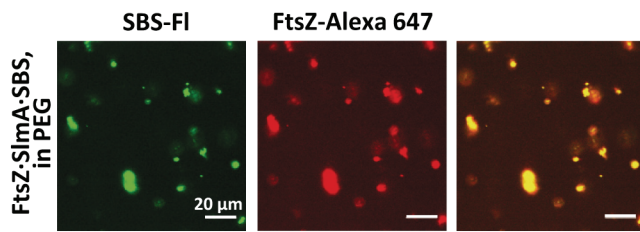


Figure S1. Formation of condensates of FtsZ-SlmA-SBS in 150 g/L PEG. The concentrations of FtsZ, SlmA and SBS were 12, 5 and 1 μ M, respectively.

Figure S2. Behavior of FtsZ at high concentration under crowding conditions. Representative confocal images showing the absence of condensates at 40 μ M FtsZ with no SlmA-SBS in 150 g/L dextran (left) or in 50 g/L PEG (right).

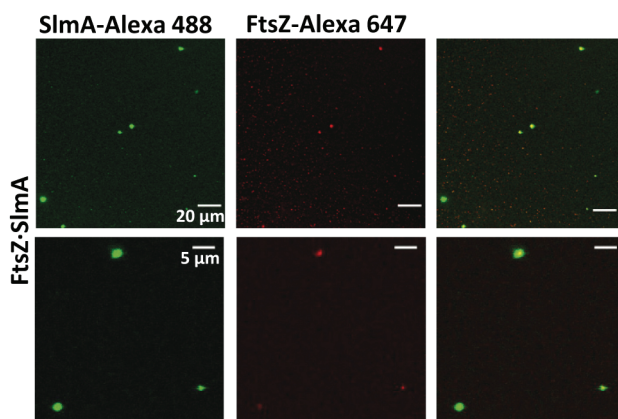
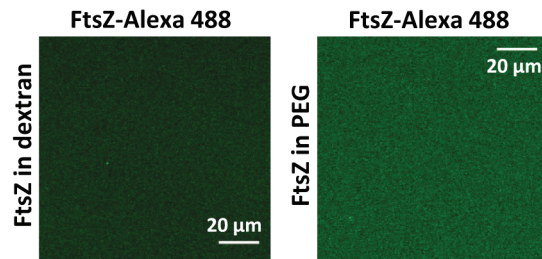
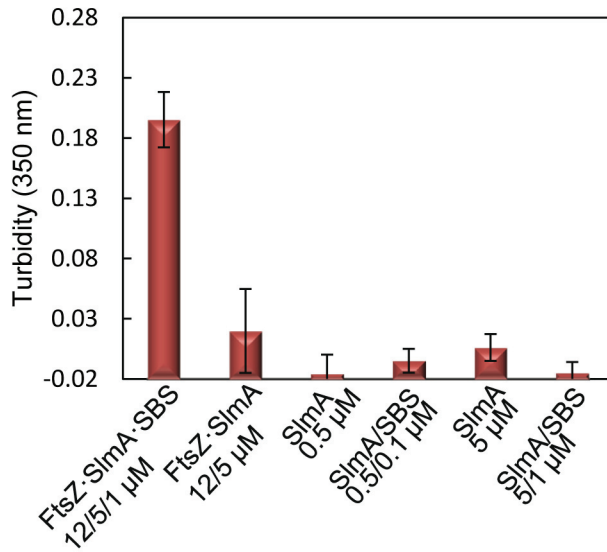
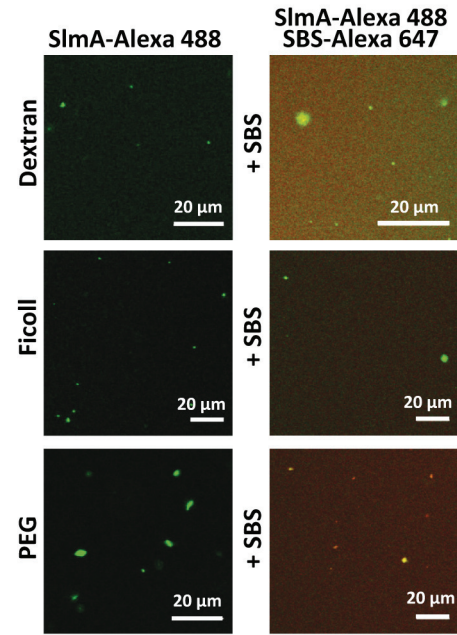


Figure S3. Condensates formed by FtsZ-SlmA in 150 g/L dextran. FtsZ and SlmA concentrations were 12 and 5 μ M, respectively.

A



B



C

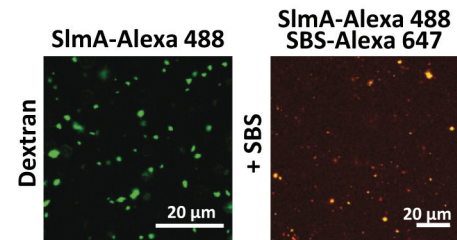


Figure S4. Formation of condensates of SlmA \pm SBS in crowding conditions. (A) Measurements of turbidity of samples containing SlmA \pm SBS in 150 g/L dextran. The samples containing FtsZ-SlmA \pm SBS at 12, 5 and 1 μM , respectively, are included as a reference. Data are the average of 2 independent experiments \pm SD, except for FtsZ-SlmA-SBS ($n = 5$). (B) SlmA condensates in the absence and presence of SBS in 150 g/L dextran or Ficoll and in 50 g/L PEG. Concentrations of SlmA and SBS were 5 and 1 μM , respectively. (C) SlmA condensates in the absence and presence of SBS in 150 g/L dextran. Concentrations of SlmA and SBS were 40 and 8 μM , respectively. All experiments in working buffer with 300 mM KCl.

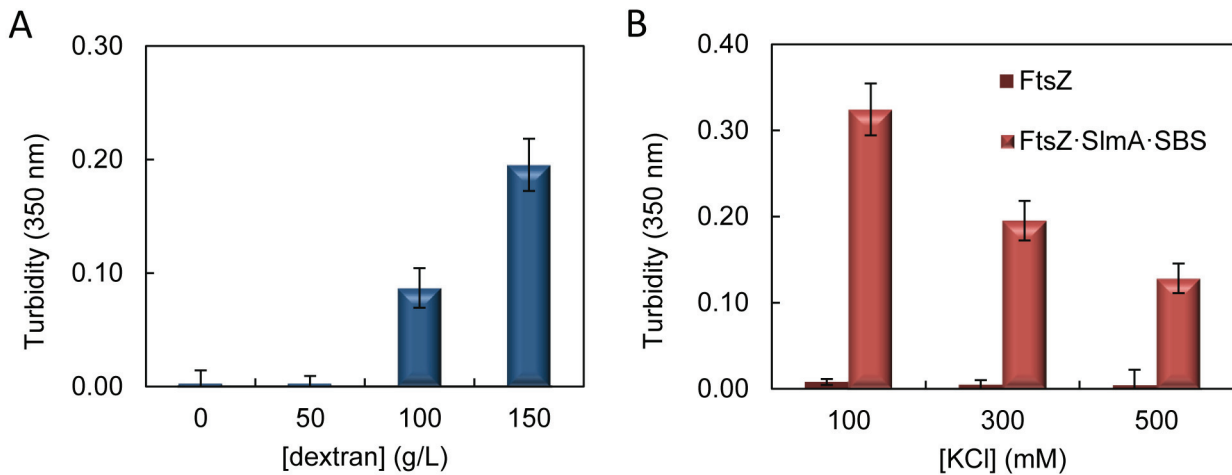


Figure S5. Dependence of the formation of FtsZ·SlmA·SBS condensates on experimental conditions as determined by turbidity. (A) Effect of dextran concentration in working buffer (300 mM KCl). Data are the average of 2 independent measurements \pm SD, except for 150 g/L dextran ($n = 5$). (B) Effect of KCl concentration in 150 g/L dextran. Data are the average of 3 independent measurements \pm SD, except for 300 mM KCl ($n = 5$). FtsZ, SlmA and SBS concentrations were 12, 5 and 1 μ M, respectively.

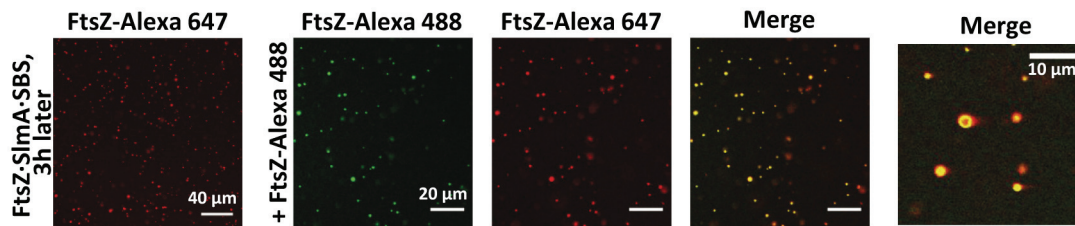


Figure S6. Dynamism of condensates of FtsZ·SlmA·SBS in dextran. Initial (far left) and final states after diffusion of FtsZ-Alexa 488 into FtsZ·SlmA·SBS condensates (FtsZ labeled with Alexa 647) 3h after complex formation in 150 g/L dextran. An image of the final estate (merge) at higher magnification is shown on the right. FtsZ, SlmA and SBS concentrations were 12, 5 and 1 μ M, respectively.

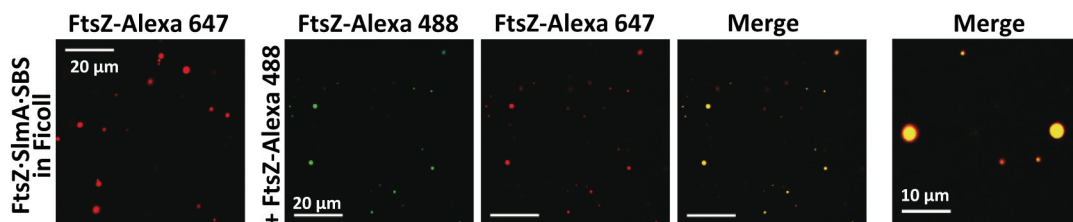


Figure S7. Dynamism of FtsZ·SlmA·SBS condensates in Ficoll. Representative confocal images showing initial (far left panel) and final states after diffusion of FtsZ-Alexa 488 into the condensates of FtsZ·SlmA·SBS containing FtsZ-Alexa 647 in 150 g/L Ficoll. An image of the final state (merge) with higher magnification is included on the right. FtsZ, SlmA and SBS concentrations were 12, 5 and 1 μ M, respectively.

Figure S8. Dynamism of condensates formed by FtsZ·SlmA in 150 g/L dextran. Final state after addition of FtsZ-Alexa 488 to FtsZ·SlmA complexes (FtsZ labeled with Alexa 647). Below, images showing the stepwise diffusion of FtsZ-Alexa 488 into the condensates at the indicated times in seconds (time zero, beginning of visualization for those particular condensates). Bottom, corresponding intensity profiles at selected times in the green channel. The profile in the red channel is shown as a reference and varies slightly among images. FtsZ and SlmA concentrations were 12 and 5 μM , respectively.

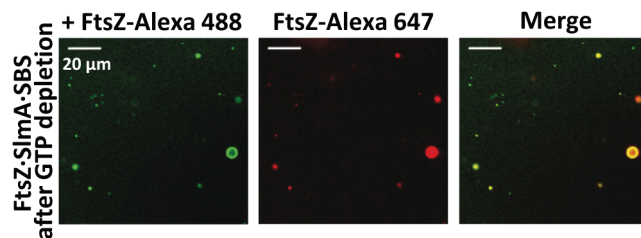
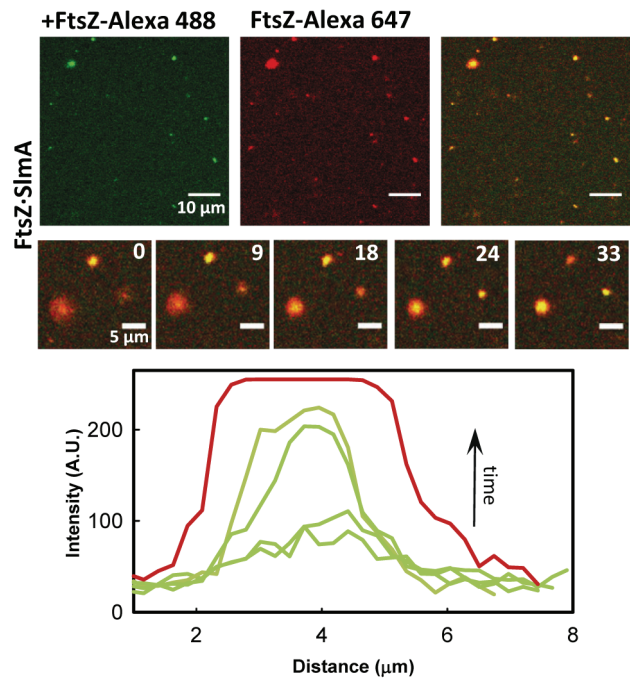


Figure S9. Dynamism of FtsZ·SlmA·SBS condensates after GTP depletion. Representative confocal images showing final state after addition of FtsZ-Alexa 488 on condensates formed by FtsZ·SlmA·SBS (FtsZ-Alexa 647) after FtsZ fibers disassembly due to GTP (0.7 mM) depletion, in 150 g/L dextran. FtsZ, SlmA and SBS concentrations were 12, 5 and 1 μM , respectively.

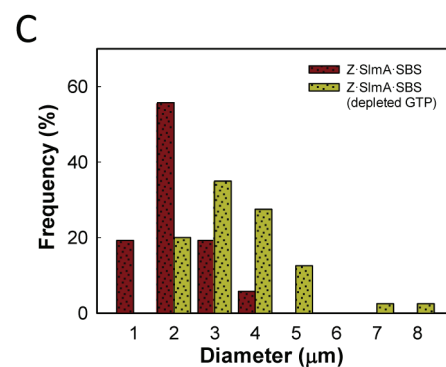
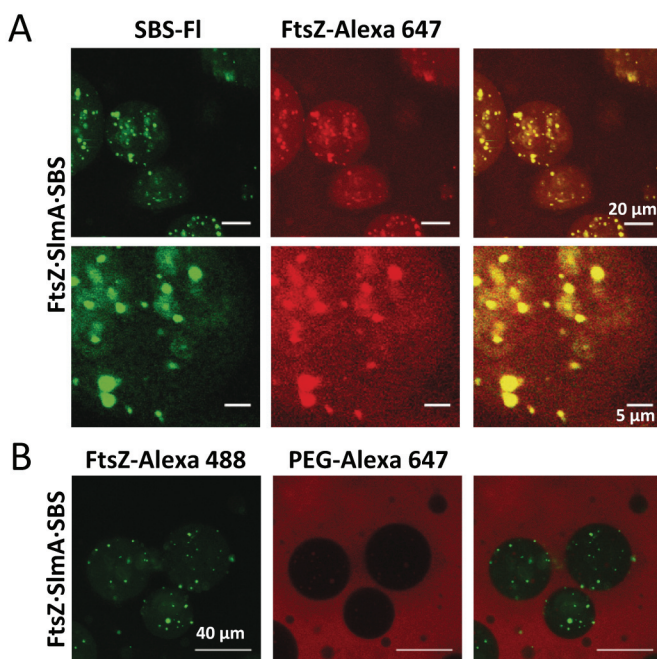


Figure S10. Formation of FtsZ·SlmA·SBS condensates in the PEG/dextran LLPS system. (A and B) Representative confocal images showing the distribution of condensates formed by FtsZ·SlmA·SBS using different labeling combinations in PEG/dextran. Concentrations of FtsZ were 6 μM (B) or 12 μM (A). SlmA and SBS, 5 and 1 μM , respectively. (C) Distribution of sizes of FtsZ·SlmA·SBS condensates before ($n = 52$) and after ($n = 40$) an FtsZ fiber assembly/disassembly cycle.

Figure S10. Formation of FtsZ·SlmA·SBS condensates in the PEG/dextran LLPS system. (A and B) Representative confocal images showing the distribution of condensates formed by FtsZ·SlmA·SBS using different labeling combinations in PEG/dextran. Concentrations of FtsZ were 6 μM (B) or 12 μM (A). SlmA and SBS, 5 and 1 μM , respectively. (C) Distribution of sizes of FtsZ·SlmA·SBS condensates before ($n = 52$) and after ($n = 40$) an FtsZ fiber assembly/disassembly cycle.

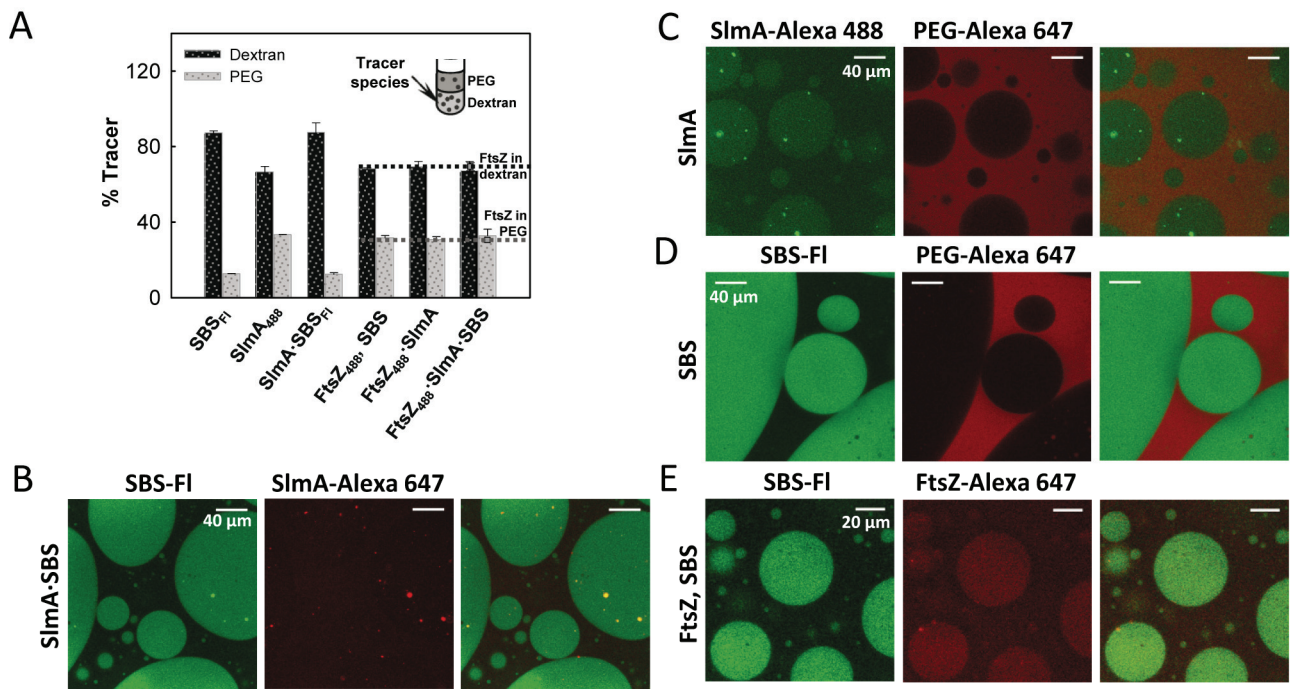


Figure S11. Distribution of division elements in the PEG/dextran LLPS system. (A) Partition of SlmA, SBS and the complexes with FtsZ within the LLPS mixture as determined by fluorescence, together with an illustration. Horizontal lines depict, for comparison, distribution within these phases of FtsZ alone. Bars represent the percentage of the fluorescently labeled element in each of the phases (dextran-rich or PEG-rich) of the sample. Reported values correspond to the average of 3 independent measurements, 6 in the case of the samples with the three components, \pm SD. Distribution of (B) SlmA-SBS complex, (C) SlmA, (D) SBS and (E) FtsZ in the presence of SBS. The concentrations of FtsZ, SlmA and SBS, when present, were 12, 5 and 1 μ M, respectively.

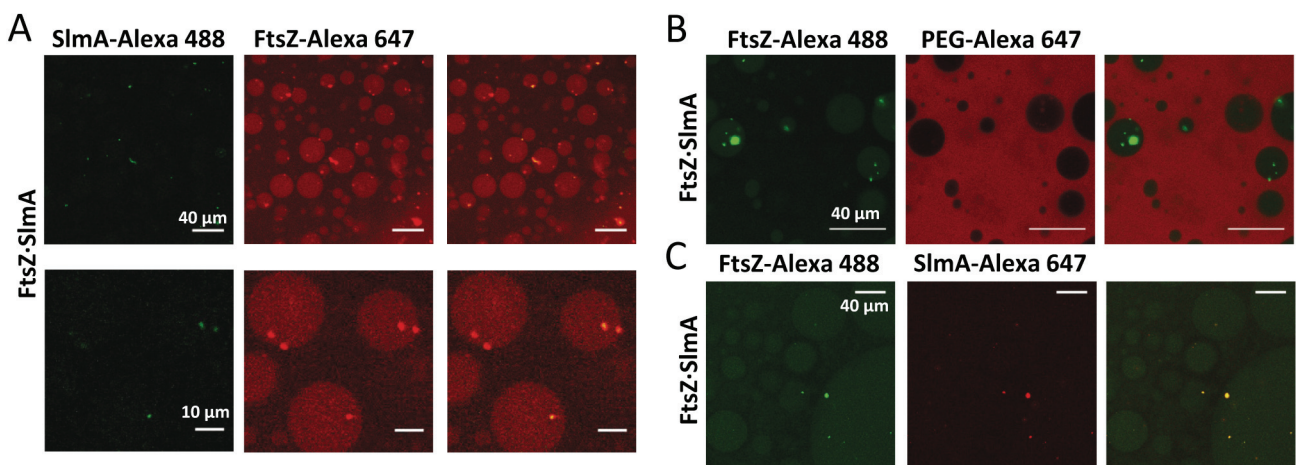


Figure S12. Formation of FtsZ-SlmA condensates in the PEG/dextran LLPS system monitored using different labeling combinations. Representative confocal images showing the distribution of condensates formed by FtsZ-SlmA in PEG/dextran. FtsZ concentrations were 6 μ M (B) or 12 μ M (A, C). SlmA, 5 μ M.

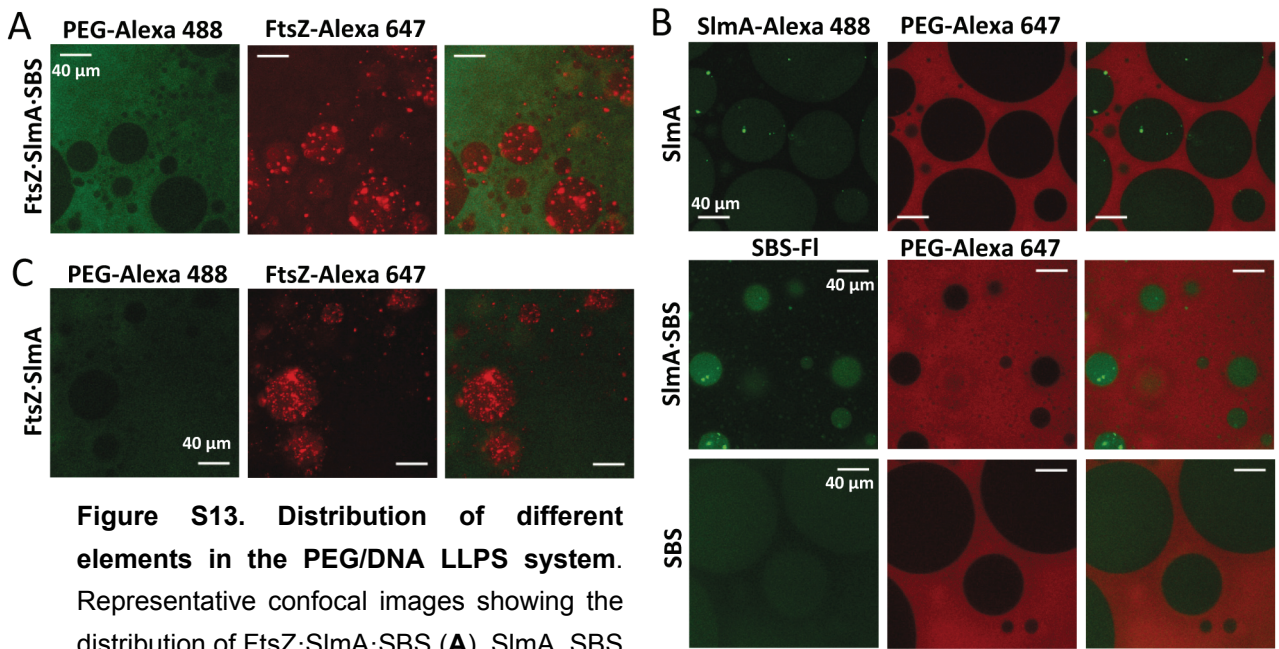


Figure S13. Distribution of different elements in the PEG/DNA LLPS system. Representative confocal images showing the distribution of FtsZ·SlmA·SBS (A), SlmA, SBS and SlmA·SBS (B) and FtsZ·SlmA (C). FtsZ, SlmA and SBS concentrations were 12, 5 and 1 μ M, respectively.

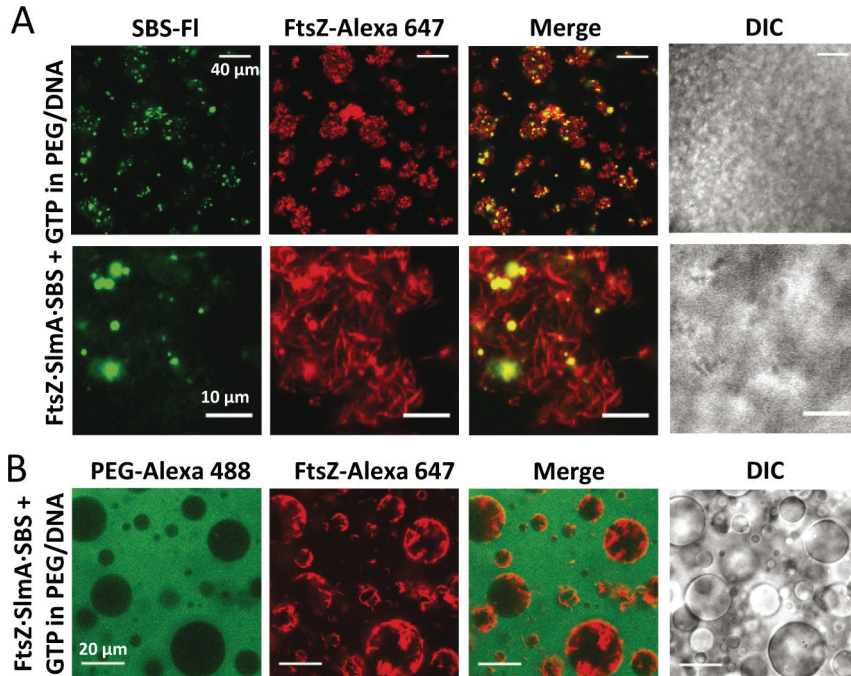


Figure S14. Fiber formation upon addition of GTP to FtsZ·SlmA·SBS condensates in the PEG/DNA LLPS system. (A) and (B) show different labeling combinations. 2 mM GTP. FtsZ, SlmA and SBS concentrations were 12, 5 and 1 μ M, respectively.

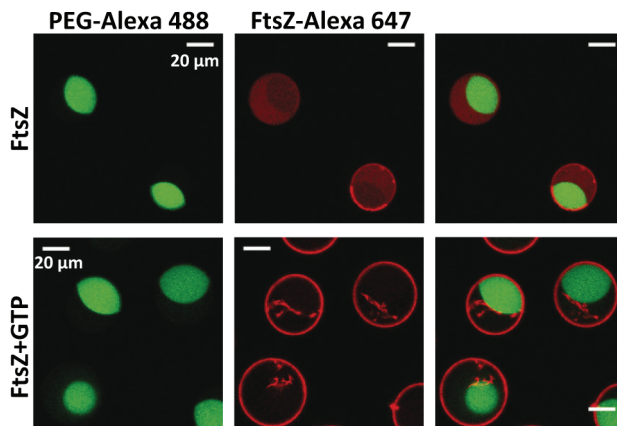


Figure S15. Microfluidic encapsulation of FtsZ in the PEG/DNA LLPS system inside microdroplets stabilized by the *E. coli* lipid mixture. Representative confocal images of the microdroplets with FtsZ (12 μ M) in the absence and presence of 1 mM GTP.

Figure S16. Control of formation of condensates with unlabeled protein or SBS. Transmitted images of FtsZ·SlmA·SBS (12 μ M/5 μ M/1 μ M) condensates in working buffer (300 mM KCl) and 150 g/L dextran.

